ICIC Express Letters
Volume **15**, Number **9**, September **2021**
 ISSN 1881-803X
pp. **961–966**

A GENERATION METHOD OF SYNTHESIZED PARALLEL-FINE-CURVE-LINE IMAGES FROM TWO IMAGES

Toru Hiraoka[1] and Kohei Inoue[2]

[1]Department of Information Systems
University of Nagasaki
1-1-1, Manabino, Nagayo-chou, Nishisonogi-gun, Nagasaki-ken 851-2195, Japan
hiraoka@sun.ac.jp

[2]Department of Communication Design Science
Kyushu University
4-9-1, Shiobaru, Minami-ku, Fukuoka-shi, Fukuoka-ken 815-8540, Japan
k-inoue@design.kyushu-u.ac.jp

Received January 2021; accepted March 2021

Abstract. *We have proposed a non-photorealistic rendering (NPR) method for generating parallel-fine-curve-line (PFCL) images using autocorrelation coefficients calculated from pixel values in the window from photographic images. PFCL patterns are uniquely determined by the characteristic of the conventional method and the change in density of photographic images. Therefore, we propose a method for synthesizing another PFCL patterns generated from other images into PFCL images. By conducting experiments using various images, we show that synthesized PFCL (S-PFCL) images are a new style of NPR and are more impressive than PFCL images.*
Keywords: Parallel-fine-curve-line image, Synthesis, Non-photorealistic rendering, Autocorrelation coefficient, Simple geometric image

1. **Introduction.** Non-photorealistic rendering (NPR) is a field in computer graphics which can create effective illustrations and appealing artistic images. Many NPR methods [1, 2, 3, 4, 5, 6, 7, 8] have been proposed for generating NPR images by image processing [9, 10] from images, videos and three-dimensional data. In the past researches, an NPR method for generating parallel-fine-curve-line (PFCL) images by an iterative image processing using correlation coefficient from photographic images has been proposed [11]. PFCL images have smooth fine curve lines aligned along edges of photographic images. Since PFCL patterns generated by the conventional method are uniquely determined by the change in density of photographic images, it is difficult to generate intentional PFCL patterns from complex photographic images. If it is possible to generate intentional PFCL patterns, the scope of use of PFCL images will expand.

In this paper, we develop a method for generating intentional synthesized PFCL (S-PFCL) images by synthesizing simple geometrical images. Intentional PFCL patterns are generated by using simple geometrical images. Furthermore, our method can generate S-PFCL images that complex photographic images are also synthesized. S-PFCL images can give an unprecedented representation of NPR. In order to show the effectiveness of our method, we experiment with various simple geometrical images and complex photographic images, and then visually verify the generated S-PFCL images.

The rest of this paper is organized as follows. Section 2 describes our method for generating S-PFCL images. Section 3 shows the experimental results, and reveals the effectiveness of our method. Finally, Section 4 concludes this paper.

DOI: 10.24507/icicel.15.09.961

2. **Our Method.** Our method generates S-PFCL images by an iterative processing using correlation coefficient with two images as input. One image is a photographic image, and the other image is a simple geometric image or a complex photographic image. Our method is implemented in two major steps. In the first step, autocorrelation coefficients are calculated for either of two images. In the second step, two input images are converted by autocorrelation coefficients. S-PFCL images are generated by repeating the two steps. A flow chart of our method is shown in Figure 1.

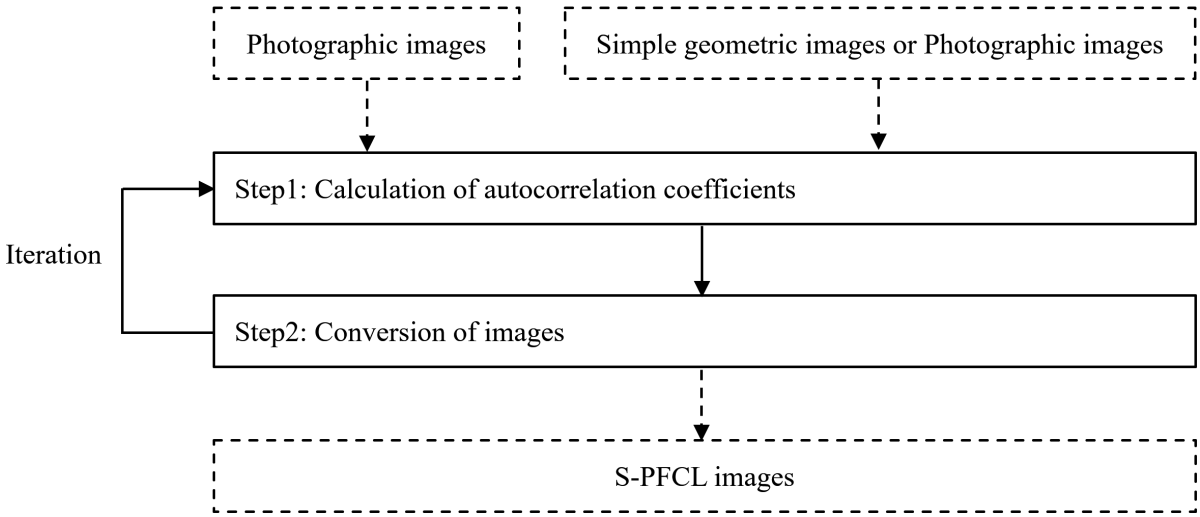

FIGURE 1. Flow chart of our method

The details of the procedure of our method are explained as follows. Pixel values in M gradations (integer values from 0 to $M-1$) of two input images of $I * J$ pixels are defined as $f_{1,i,j}$ and $f_{2,i,j}$ $(i = 1, 2, \ldots, I;\ j = 1, 2, \ldots, J)$, respectively.

In the first step, correlation coefficients are calculated using pixel values $f^{(t)}_{1,i,j}$ and $f^{(t)}_{2,i,j}$ in the window of $2W+1$ centered on the pixel (i, j), where t $(= 1, 2, \ldots)$ is the number of iterations, $f^{(1)}_{1,i,j} = f_{1,i,j}$, and $f^{(1)}_{2,i,j} = f_{2,i,j}$. The averages $a^{(t)}_{1,i,j}$ and $a^{(t)}_{2,i,j}$ of the pixel values in the window are respectively calculated as follows.

$$a^{(t)}_{1,i,j} = \frac{\sum_{k=-W}^{W} \sum_{l=-W}^{W} f^{(t)}_{1,i+k,j+l}}{(2W+1)^2} \tag{1}$$

$$a^{(t)}_{2,i,j} = \frac{\sum_{k=-W}^{W} \sum_{l=-W}^{W} f^{(t)}_{2,i+k,j+l}}{(2W+1)^2} \tag{2}$$

Vectors $\vec{v}^{(t)}_{1,1,i,j}$ and $\vec{v}^{(t)}_{1,2,i,j}$ are created by arranging the pixel values in the window as follows.

$$\begin{aligned} \vec{v}^{(t)}_{1,1,i,j} = \Big(& f^{(t)}_{1,i-W,j-W} - a^{(t)}_{1,i,j}, f^{(t)}_{1,i-W+1,j-W} - a^{(t)}_{1,i,j}, f^{(t)}_{1,i-W+2,j-W} - a^{(t)}_{1,i,j}, \ldots, \\ & f^{(t)}_{1,i-2,j} - a^{(t)}_{1,i,j}, f^{(t)}_{1,i-1,j} - a^{(t)}_{1,i,j}, f^{(t)}_{1,i,j} - a^{(t)}_{1,i,j}, f^{(t)}_{1,i+1,j} - a^{(t)}_{1,i,j}, f^{(t)}_{1,i+2,j} - a^{(t)}_{1,i,j}, \\ & \ldots, f^{(t)}_{1,i+W-2,j+W} - a^{(t)}_{1,i,j}, f^{(t)}_{1,i+W-1,j+W} - a^{(t)}_{1,i,j}, f^{(t)}_{1,i+W,j+W} - a^{(t)}_{1,i,j} \Big) \end{aligned} \tag{3}$$

$$\begin{aligned} \vec{v}^{(t)}_{1,2,i,j} = \Big(& f^{(t)}_{2,i-W,j-W} - a^{(t)}_{2,i,j}, f^{(t)}_{2,i-W+1,j-W} - a^{(t)}_{2,i,j}, f^{(t)}_{2,i-W+2,j-W} - a^{(t)}_{2,i,j}, \ldots, \\ & f^{(t)}_{2,i-2,j} - a^{(t)}_{2,i,j}, f^{(t)}_{2,i-1,j} - a^{(t)}_{2,i,j}, f^{(t)}_{2,i,j} - a^{(t)}_{2,i,j}, f^{(t)}_{2,i+1,j} - a^{(t)}_{2,i,j}, f^{(t)}_{2,i+2,j} - a^{(t)}_{2,i,j}, \\ & \ldots, f^{(t)}_{2,i+W-2,j+W} - a^{(t)}_{2,i,j}, f^{(t)}_{2,i+W-1,j+W} - a^{(t)}_{2,i,j}, f^{(t)}_{2,i+W,j+W} - a^{(t)}_{2,i,j} \Big) \end{aligned} \tag{4}$$

Vectors $\vec{v}^{(t)}_{2,1,i,j}$ and $\vec{v}^{(t)}_{2,2,i,j}$ are created by inverting the elements of vectors $\vec{v}^{(t)}_{1,1,i,j}$ and $\vec{v}^{(t)}_{1,2,i,j}$ as follows.

$$\begin{aligned}\vec{v}^{(t)}_{2,1,i,j} = \Big(&f^{(t)}_{1,i+W,j+W} - a^{(t)}_{1,i,j}, f^{(t)}_{1,i+W-1,j+W} - a^{(t)}_{1,i,j}, f^{(t)}_{1,i+W-2,j+W} - a^{(t)}_{1,i,j}, \ldots, \\ &f^{(t)}_{1,i+2,j} - a^{(t)}_{1,i,j}, f^{(t)}_{1,i+1,j} - a^{(t)}_{1,i,j}, f^{(t)}_{1,i,j} - a^{(t)}_{1,i,j}, f^{(t)}_{1,i-1,j} - a^{(t)}_{1,i,j}, f^{(t)}_{1,i-2,j} - a^{(t)}_{1,i,j}, \\ &\ldots, f^{(t)}_{1,i-W+2,j-W} - a^{(t)}_{1,i,j}, f^{(t)}_{1,i-W+1,j-W} - a^{(t)}_{1,i,j}, f^{(t)}_{1,i-W,j-W} - a^{(t)}_{1,i,j}\Big)\end{aligned} \tag{5}$$

$$\begin{aligned}\vec{v}^{(t)}_{2,2,i,j} = \Big(&f^{(t)}_{2,i+W,j+W} - a^{(t)}_{2,i,j}, f^{(t)}_{2,i+W-1,j+W} - a^{(t)}_{2,i,j}, f^{(t)}_{2,i+W-2,j+W} - a^{(t)}_{2,i,j}, \ldots, \\ &f^{(t)}_{2,i+2,j} - a^{(t)}_{2,i,j}, f^{(t)}_{2,i+1,j} - a^{(t)}_{2,i,j}, f^{(t)}_{2,i,j} - a^{(t)}_{2,i,j}, f^{(t)}_{2,i-1,j} - a^{(t)}_{2,i,j}, f^{(t)}_{2,i-2,j} - a^{(t)}_{2,i,j}, \\ &\ldots, f^{(t)}_{2,i-W+2,j-W} - a^{(t)}_{2,i,j}, f^{(t)}_{2,i-W+1,j-W} - a^{(t)}_{2,i,j}, f^{(t)}_{2,i-W,j-W} - a^{(t)}_{2,i,j}\Big)\end{aligned} \tag{6}$$

Correlation coefficients $c^{(t)}_{1,i,j}$ and $c^{(t)}_{2,i,j}$ are calculated using vectors $\vec{v}^{(t)}_{1,1,i,j}$, $\vec{v}^{(t)}_{2,1,i,j}$, $\vec{v}^{(t)}_{1,2,i,j}$, and $\vec{v}^{(t)}_{2,2,i,j}$ as follows.

$$c^{(t)}_{1,i,j} = \frac{\vec{v}^{(t)}_{1,1,i,j} \cdot \vec{v}^{(t)}_{2,1,i,j}}{\left|\vec{v}^{(t)}_{1,1,i,j}\right| \left|\vec{v}^{(t)}_{2,1,i,j}\right|} \tag{7}$$

$$c^{(t)}_{2,i,j} = \frac{\vec{v}^{(t)}_{1,2,i,j} \cdot \vec{v}^{(t)}_{2,2,i,j}}{\left|\vec{v}^{(t)}_{1,2,i,j}\right| \left|\vec{v}^{(t)}_{2,2,i,j}\right|} \tag{8}$$

In the second step, the pixel values $f^{(t+1)}_{1,i,j}$ and $f^{(t+1)}_{2,i,j}$ using correlation coefficients $c^{(t)}_{1,i,j}$ and $c^{(t)}_{2,i,j}$ are converted as

$$f^{(t+1)}_{1,i,j} = f_{1,i,j} + bc^{(t)}_{2,i,j} \tag{9}$$

$$f^{(t+1)}_{2,i,j} = f_{2,i,j} + bc^{(t)}_{1,i,j} \tag{10}$$

where b is a positive constant. The pixel values $f^{(t+1)}_{1,i,j}$ and $f^{(t+1)}_{2,i,j}$ are set to 0 if the values are less than 0, and are respectively set to $M-1$ if the values are greater than $M-1$.

Steps 1 and 2 are repeated T times. S-PFCL images are composed of the pixel values $f^{(T)}_{1,i,j}$.

3. **Experiments.** We visually confirmed S-PFCL images using Lenna image shown in Figure 2 and four simple geometric images shown in Figure 3. All images were $512 * 512$ pixels and 256 gradation. Referring to [11] in all experiments, the parameters W, b, and T were set to 4, 100, and 10, respectively. The results of the experiment are shown in Figure 4. To make the details of S-PFCL patterns easier to see, the enlarged view of S-PFCL image on the left edge of Figure 4 is shown in Figure 5. S-PFCL patterns could

FIGURE 2. Lenna image

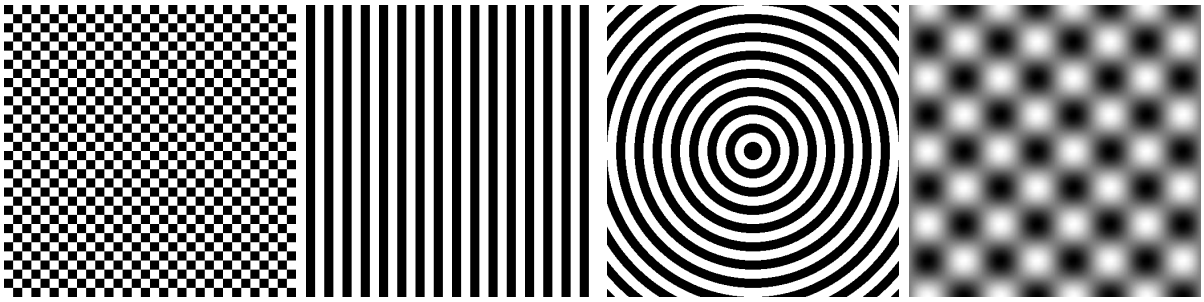

FIGURE 3. Simple geometric images

FIGURE 4. S-PFCL images using simple geometric images

FIGURE 5. Enlarged view of the left edge of Figure 4

be changed according to simple geometric images. In addition, S-PFCL images giving a different impression compared to PFCL images could be generated. For reference, Figure 7 shows S-PFCL images that four simple geometric images are synthesized into other photographic images shown in Figure 6. All images in Figure 6 were $512 * 512$ pixels and 256 gradation.

FIGURE 6. Photographic images

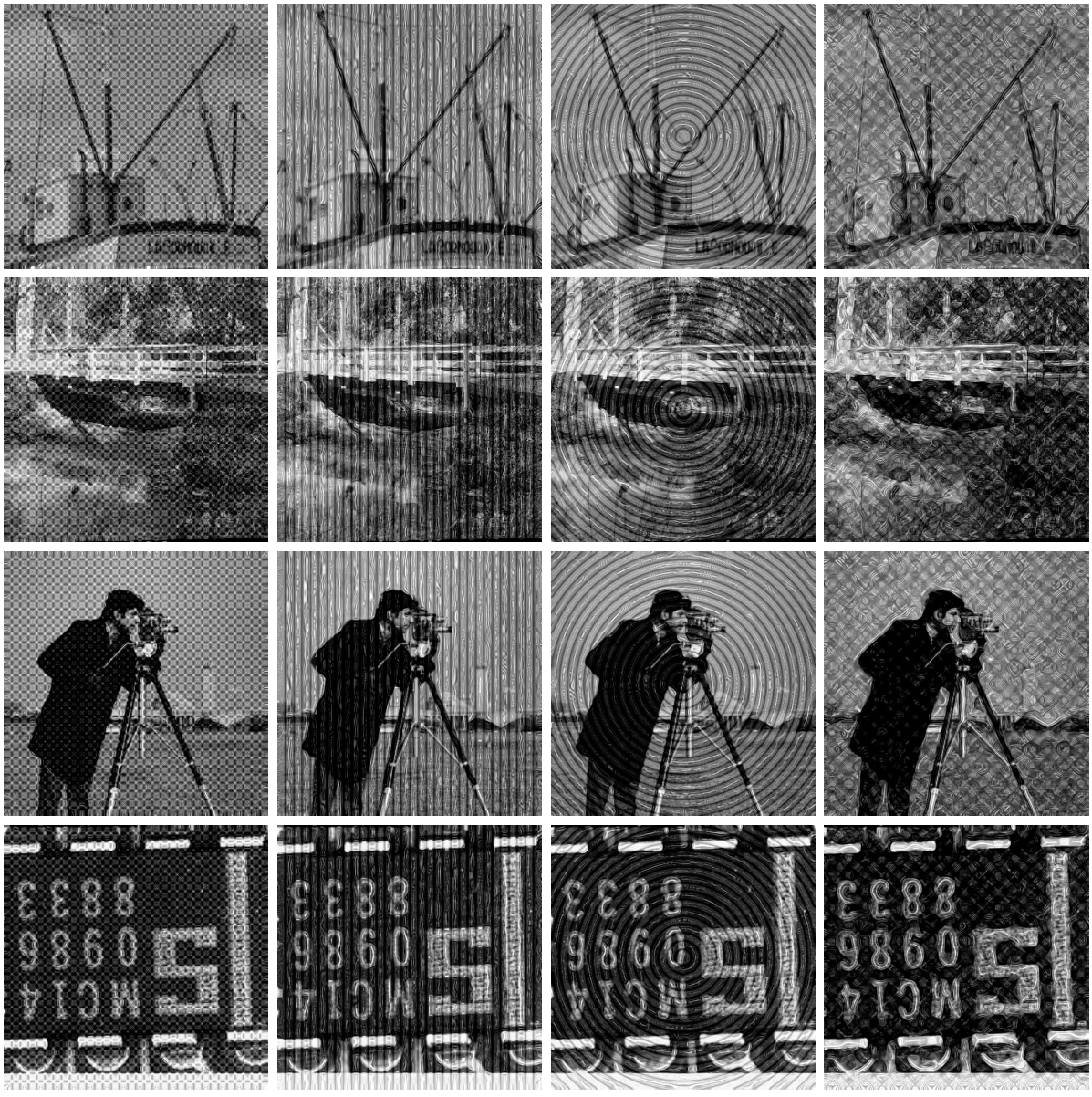

FIGURE 7. S-PFCL images using simple geometric images from various photographic images

We visually confirmed S-PFCL images using Lenna image and four complex photographic images shown in Figure 6. The parameters W, b, and T were set to 4, 100, and 10, respectively. The results of the experiment are shown in Figure 8. Our method could also synthesize complex photographic images.

FIGURE 8. S-PFCL images using complex photographic images

4. **Conclusions.** We proposed an NPR method for generating S-PFCL images by an iterative processing using correlation coefficient with two images as input. We demonstrated the effectiveness of our method through experiments using photographic images and simple geometric images. The experimental results show that our method can synthesize another PFCL patterns generated from other images into PFCL images. Then, our method could generate S-PFCL images with an impression different from PFCL images.

In future work, we will try to apply our method to color photographic images and videos.

Acknowledgment. This work was supported by JSPS KAKENHI Grant Number JP19K 12664.

REFERENCES

[1] P. Haeberli, Paint by numbers: Abstract image representations, *ACM SIGGRAPH Computer Graphics*, vol.24, no.4, pp.207-214, 1990.

[2] D. D. Seligmann and S. Feiner, Automated generation of intent-based 3D illustrations, *ACM SIGGRAPH Computer Graphics*, vol.25, no.4, pp.123-132, 1991.

[3] J. Lansdown and S. Schofield, Expressive rendering: A review of nonphotorealistic techniques, *IEEE Computer Graphics and Applications*, vol.15, no.3, pp.29-37, 1995.

[4] W. Qian, D. Xu, K. Yue, Z. Guan, Y. Pu and Y. Shi, Gourd pyrography art simulating based on non-photorealistic rendering, *Multimedia Tools and Applications*, vol.76, no.13, pp.14559-14579, 2017.

[5] D. Martin, G. Arroyo, A. Rodriguez and T. Isenberg, A survey of digital stippling, *Computers & Graphics*, vol.67, pp.24-44, 2017.

[6] Q. Shen, D. Cui, Y. Sheng and G. Zhang, Illumination-preserving embroidery simulation for non-photorealistic rendering, *International Conference on Multimedia Modeling 2017*, pp.233-244, 2017.

[7] T. Lindemeier, J. M. Gulzow and O. Deussen, Painterly rendering using limited paint color palettes, *Proc. of the Conference on Vision, Modeling, and Visualization 2018*, pp.135-145, 2018.

[8] W. Qian, D. Xu, J. Cao, Z. Guan and Y. Pu, Aesthetic art simulation for embroidery style, *Multimedia Tools and Applications*, vol.78, no.1, pp.995-1016, 2019.

[9] H.-D. Lin, C.-Y. Lin and C.-H. Lin, Detection of fishbones in fish floss products using curvelet transform based square-ring band-highpass filtering techniques, *International Journal of Innovative Computing, Information and Control*, vol.17, no.1, pp.31-47, 2021.

[10] P. Lu, Y. Ding and C. Wang, Multi-small target detection and tracking based on improved YOLO and SIFT for drones, *International Journal of Innovative Computing, Information and Control*, vol.17, no.1, pp.205-224, 2021.

[11] T. Hiraoka, T. Katayama and K. Urahama, Generation of parallel-fine-curve-line images by iterative calculation using correlation coefficient, *ICIC Express Letters*, vol.12, no.11, pp.1131-1136, 2018.